

# Structural basis for the enantiospecificities of *R*- and *S*-specific phenoxypropionate/ $\alpha$ -ketoglutarate dioxygenases

TINA A. MÜLLER,<sup>1</sup> MARIA I. ZAVODSZKY,<sup>2</sup> MICHAEL FEIG,<sup>2,3</sup> LESLIE A. KUHN,<sup>2</sup>  
AND ROBERT P. HAUSINGER<sup>1,2</sup>

Departments of <sup>1</sup>Microbiology & Molecular Genetics, <sup>2</sup>Biochemistry & Molecular Biology, and <sup>3</sup>Chemistry, Michigan State University, East Lansing, Michigan 48824-4320, USA

(RECEIVED December 21, 2005; FINAL REVISION March 15, 2006; ACCEPTED March 19, 2006)

## Abstract

(*R*)- and (*S*)-dichlorprop/ $\alpha$ -ketoglutarate dioxygenases (RdpA and SdpA) catalyze the oxidative cleavage of 2-(2,4-dichlorophenoxy)propanoic acid (dichlorprop) and 2-(4-chloro-2-methyl-phenoxy)propanoic acid (mecoprop) to form pyruvate plus the corresponding phenol concurrent with the conversion of  $\alpha$ -ketoglutarate ( $\alpha$ KG) to succinate plus CO<sub>2</sub>. RdpA and SdpA are strictly enantiospecific, converting only the (*R*) or the (*S*) enantiomer, respectively. Homology models were generated for both enzymes on the basis of the structure of the related enzyme TauD (PDB code 1OS7). Docking was used to predict the orientation of the appropriate mecoprop enantiomer in each protein, and the predictions were tested by characterizing the activities of site-directed variants of the enzymes. Mutant proteins that changed at residues predicted to interact with (*R*)- or (*S*)-mecoprop exhibited significantly reduced activity, often accompanied by increased *K<sub>m</sub>* values, consistent with roles for these residues in substrate binding. Four of the designed SdpA variants were (slightly) active with (*R*)-mecoprop. The results of the kinetic investigations are consistent with the identification of key interactions in the structural models and demonstrate that enantiospecificity is coordinated by the interactions of a number of residues in RdpA and SdpA. Most significantly, residues Phe171 in RdpA and Glu69 in SdpA apparently act by hindering the binding of the wrong enantiomer more than the correct one, as judged by the observed decreases in *K<sub>m</sub>* when these side chains are replaced by Ala.

**Keywords:** dioxygenase; enantiospecificity; mecoprop; site-directed mutagenesis; structural modeling; docking

**Supplemental material:** see [www.proteinscience.org](http://www.proteinscience.org)

Reprint requests to: Robert P. Hausinger, Department of Microbiology and Molecular Genetics, 6193 Biomedical Physical Sciences, Michigan State University, East Lansing, MI 48824-4320, USA; e-mail: [hausinge@msu.edu](mailto:hausinge@msu.edu); fax: (517) 353-8957.

**Abbreviations:** 2,4-D, 2,4-dichlorophenoxyacetic acid; AlkB, alkylation-damaged DNA repair enzyme; AtsK, alkyl sulfatase; ANS, anthocyanidin synthase; CarC, carbapenam synthase; CAS, clavaminic synthase; CSD, Cambridge Structural Database; DAOCS, deacetoxycephalosporin C synthase; dichlorprop, 2-(2,4-dichlorophenoxy)propanoic acid; FIH, factor inhibiting hypoxia-inducible factor;  $\alpha$ KG,  $\alpha$ -ketoglutarate; mecoprop, 2-(4-chloro-2-methyl-phenoxy)propanoic acid; NTA, nitrilotriacetic acid; PAHX, phytanoyl-coenzyme A 2-hydroxylase; PDB, Protein Data Bank; RdpA, (*R*)-specific dichlorprop/ $\alpha$ KG dioxygenase; SdpA, (*S*)-specific dichlorprop/ $\alpha$ KG dioxygenase; TfdA, 2,4-D/ $\alpha$ KG dioxygenase; TauD, taurine/ $\alpha$ KG dioxygenase; TR, tropinone reductase; SDS-PAGE, sodium dodecyl sulfate-polyacrylamide gel electrophoresis.

Article and publication are at <http://www.proteinscience.org/cgi/doi/10.1110/ps.052059406>.

Phenoxyalkanoic acids are systemic and post-emergence inhibitors of broadleaf weeds and are among the most widely applied herbicides in the world (Worthing and Hance 1991; Ahrens 1994; Donaldson et al. 2002). These synthetic auxins (Åberg 1973; Loos 1975; Ahrens 1994) include 2,4-dichlorophenoxyacetic acid (2,4-D) along with the chiral representatives 2-(2,4-dichlorophenoxy)propanoic acid (dichlorprop) and 2-(4-chloro-2-methyl-phenoxy)propanoic acid (mecoprop), of which only the (*R*)-enantiomers are herbicidally active (Matell 1953). Microorganisms able to degrade these phenoxyalkanoic acid herbicides have been isolated from different environments, and their degradative pathways have been elucidated (Zipper et al. 1996; Hausinger et al. 1997; Tett et al. 1997;

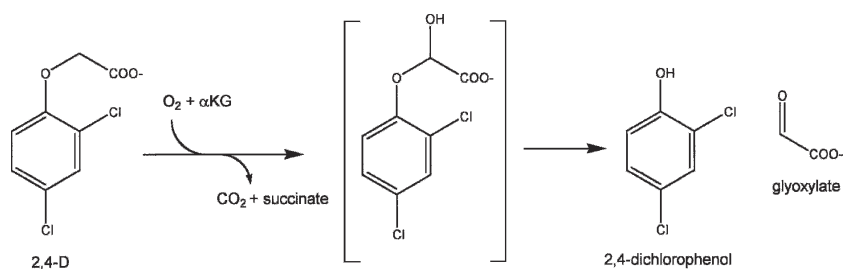
Müller et al. 1999, 2001). For example, the first step in 2,4-D metabolism is side-chain hydroxylation to form an unstable intermediate that decomposes by elimination of the phenol derivative (Scheme 1).

The 2,4-D hydroxylase (TfdA) from *Cupriavidus necator* (formerly *Ralstonia eutropha*) JMP134(pJP4) has been intensively studied and shown to require Fe<sup>II</sup> as a cofactor and  $\alpha$ -ketoglutarate ( $\alpha$ KG) as a cosubstrate (Fukumori and Hausinger 1993a,b; Saari and Hausinger 1998; Hegg et al. 1999; Hogan et al. 2000; Dunning Hotopp and Hausinger 2002). For mecoprop or dichlorprop metabolism, best studied in the soil bacterium *Sphingomonas herbicidovorans* MH, the enantiomers are separately transported into the cell by distinct uptake systems (Nickel et al. 1997), and enantiomer-specific (*R*)- and (*S*)-dichlorprop/ $\alpha$ KG dioxygenases (RdpA and SdpA) catalyze the initial degradation steps as illustrated in Scheme 2 (Nickel et al. 1997; Müller 2004; Müller et al. 2004b). RdpA and SdpA share 30% amino acid sequence identity to each other and 30% and 37% identity, respectively, to TfdA, with no significant gaps in alignment quality, indicating that they are all close structural homologs (Sander and Schneider 1991). The substituted phenol products released from these Fe<sup>II</sup>/ $\alpha$ KG-dependent dioxygenases are subsequently converted to the corresponding catechols and further metabolized by the modified *ortho*-cleavage pathway.

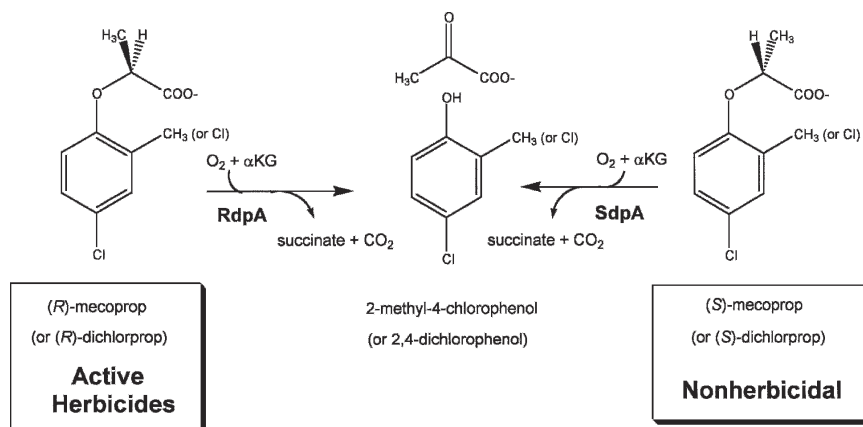
The herbicide-degrading dioxygenases belong to a large family of mononuclear, nonheme Fe<sup>II</sup> enzymes that catalyze a broad array of reactions (for review, see Hausinger 2004; Clifton et al. 2006) including hydroxylations, epoxidations, desaturations, ring formation, ring expansion, and as only recently discovered, chlorinations (Vaillancourt et al. 2005a,b). Crystal structures have been elucidated for several family members including taurine/ $\alpha$ KG dioxygenase (TauD) (Elkins et al. 2002; O'Brien et al. 2003), alkyl sulfatase (AtsK) (Müller et al. 2004a, 2005), clavaminic synthase (CAS) (Zhang et al. 2000), deacetoxycephalosporin C synthase (DAOCS) (Valegård et al. 1998), anthocyanidin synthase (ANS) (Wilmouth et al. 2002), carbapenam synthase (CarC) (Clifton et al. 2003), proline 3-hydroxylase (Clifton et al. 2001), the factor inhibiting hypoxia-inducible factor (FIH) (Dann et al. 2002; Elkins et al. 2003), phytanoyl-

coenzyme A 2-hydroxylase (PAHX) (McDonough et al. 2005), and the DNA repair enzyme AlkB (Yu et al. 2006). The structures reveal a common  $\beta$ -jelly roll or double-stranded  $\beta$ -helix fold containing a metal ion-binding motif: His<sup>1</sup>-X-Asp/Glu-X<sub>n</sub>-His<sup>2</sup> (where *n* varies from 40 to 153 residues). Three water molecules occupy the remaining metal ligand positions in the resting enzyme. Two water molecules are displaced upon binding of the cosubstrate, with the  $\alpha$ KG C-2 keto group coordinating opposite the carboxylate side chain and the  $\alpha$ KG C-1 carboxyl group binding opposite either His<sup>1</sup> (TauD, AtsK, CAS, and FIH) or opposite His<sup>2</sup> (DAOCS, ANS, CarC, PAHX, and AlkB), with a nearby Arg residue (located 15–22 residues beyond His<sup>2</sup> in the sequence) providing additional stabilization to the C-1 carboxylate in the cases of TauD, AtsK, CAS, CarC, and AlkB. Another Arg residue (located in the sequence about 10 residues beyond His<sup>2</sup>) is positioned to form an ion pair with the C-5 carboxylate of  $\alpha$ KG in all structures except FIH, where a Lys located elsewhere in the sequence provides stabilization. Unlike other Fe<sup>II</sup> sites, the  $\alpha$ KG-bound metalcenters exhibit a characteristic metal-to-ligand charge-transfer transition (Pavel et al. 1998; Hegg et al. 1999; Ryle et al. 1999; Trewick et al. 2002) conferring a lilac color to this state of the enzymes. The primary substrate (e.g., taurine in the case of TauD) does not bind to the metal center, but the aforementioned crystallographic studies and additional spectroscopic evidence (Ho et al. 2001; Zhou et al. 2001) indicate that substrate binding leads to the loss of the final water molecule, thus creating a site for binding of oxygen. In the case of TauD, oxidative decarboxylation of  $\alpha$ KG has been shown to produce an Fe<sup>IV</sup>-oxo intermediate species that inserts oxygen into the unactivated C–H bond (Price et al. 2003a,b, 2005; Proshlyakov et al. 2004; Riggs-Gelasco et al. 2004; Grzyska et al. 2005).

Sequence alignments highlight several potential key residues of the (*R*)- and (*S*)-dichlorprop/ $\alpha$ KG dioxygenases from *S. herbicidovorans* MH (Müller 2004). The His<sup>1</sup>-X-Asp/Glu-X<sub>n</sub>-His<sup>2</sup> motif of RdpA is comprised of residues His111, Asp113, and His270, while that of SdpA involves His102, Asp104, and His257. Fifteen residues beyond His<sup>2</sup> are residues predicted to interact with the C-1 carboxylate of  $\alpha$ KG, Arg285 and His272, respectively.



Scheme 1.



Scheme 2.

Furthermore, Arg281 and Arg268 of the two proteins are predicted to form salt bridges to the  $\alpha$ KG C-5 carboxylate, with additional interactions involving Thr138 of RdpA and Thr129 of SdpA. In contrast to these conserved residues, essentially nothing is known about the phenoxypropanoic acid-binding sites of these proteins, especially with regard to the structural basis of enantiospecificity.

Here, we describe the construction of homology models of SdpA and RdpA from *S. herbicidovorans* MH and the use of docking to identify residues likely to be involved in herbicide binding. Previous homology models have led to successes in elucidating or designing specificity-conferring interactions in ligands. For instance, homology modeling of a cercarial (human parasite) elastase led to the development of an effective elastase inhibitor (Cohen et al. 1991) and to understanding the specificity determinants for ligands binding to a parasite tRNA synthetase versus its human homolog (Sukuru et al. 2006). Here, we test by site-directed mutagenesis and kinetic analysis the residues predicted to be involved in substrate binding, enantiospecificity, or catalysis. The activity experiments are consistent with the key residues identified by modeling being involved in substrate binding. We provide additional evidence that several amino acids are responsible for the enantiospecificity of RdpA and SdpA, demonstrate that the active site of SdpA is less specific than RdpA for its substrate, and discuss the structural implications of these results.

## Results

### *SdpA and RdpA homology models*

RdpA and SdpA were aligned with TauD (Supplemental Fig. S1), and homology models were created as described in Materials and Methods (Supplemental Fig. S2) using

the TauD structure as a structural template (O'Brien et al. 2003). The two phenoxypropionate-degrading proteins are predicted to contain jelly roll or double-stranded  $\beta$ -helix folds comprised of eight  $\beta$ -strands with connecting loops, as is typical of this enzyme family (Hausinger 2004; Clifton et al. 2006). The homology models contain  $\text{Fe}^{\text{II}}$ -binding sites (His111, Asp113, and His270 in RdpA or His102, Asp104, and His257 in SdpA), as expected from former sequence alignments with other  $\text{Fe}^{\text{II}}$ / $\alpha$ KG-dependent dioxygenases (Müller 2004). The high degree of active-site sequence identity and strong orientation of key side chains by interactions with the  $\text{Fe}^{\text{II}}$  are supportive of the active site being the most conserved and structurally accurate part of the RdpA and SdpA models. Detailed analysis of favored  $\alpha$ KG-binding motifs in other members of this enzyme family indicate the iron is chelated by  $\alpha$ KG with its keto group positioned opposite Asp113 of RdpA or Asp104 of SdpA and its C-1 carboxylate located so as to interact with His111 and His102, respectively. The positively charged residues Arg285 in RdpA and His272 in SdpA are well positioned to provide additional stabilization of the  $\alpha$ KG C-1 carboxylate, and, in each protein, the C-5 carboxylate of  $\alpha$ KG forms a salt bridge with Arg268 and Arg281, respectively. Whereas the RdpA structure represents only one subunit of the predicted trimeric protein, SdpA is suggested to be monomeric, based on gel-filtration experiments (Müller 2004).

### *Docking of substrates into the RdpA and SdpA structures*

The natural substrates (R)- and (S)-mecoprop were docked into the active sites of RdpA and SdpA to gain insight into the basis of enzyme enantiospecificity. First, the cosubstrate  $\alpha$ KG was modeled into the active sites of RdpA and SdpA using two distinct conformations, as found in the crystal structures of  $\text{Fe}^{\text{II}}$ / $\alpha$ KG-dependent dioxygenases

(Clifton et al. 2006). The flat conformation has the five-member ring formed by the metal chelate coplanar with the C-5 carboxylate, whereas the twist conformation has the two planes forming a 90° angle. The resulting four models were energy-minimized and used as targets for substrate docking with the program SLIDE (Zavodszky et al. 2002) with the assumption that the substrate carbon undergoing hydroxylation would be located approximately at the same position relative to the iron center as the key carbon atom of taurine in TauD (Elkins et al. 2002; O'Brien et al. 2003). The mecoprop-docking interactions with RdpA and SdpA were analyzed in detail, and one model of each protein was selected based on the most favorable interactions between enzyme and substrate (see below). These models are illustrated in Figure 1, with the corresponding plots of mecoprop interactions shown in Figure 2.

#### Binding of (*R*)-mecoprop to RdpA

The substrate (*R*)-mecoprop consists of a hydrophobic phenoxy ring and a polar propanoic acid, with both components needing to be accommodated and bound by the active site. The  $\alpha$ KG conformation leading to the most favorable interactions has  $\alpha$ KG in the twist confor-

mation and positions the phenoxy ring of (*R*)-mecoprop as illustrated in Figure 1A (with the corresponding interactions plotted in Fig. 2A). The mecoprop carboxylate interacts with the amide nitrogen of Ser114, the hydroxyl group of Tyr221, and a guanidino nitrogen of Arg285. The Tyr221 hydroxyl group also is predicted to lie near (3.5 Å) the substrate ether oxygen atom and could play a role in directing enantiospecificity. Residues lining the hydrophobic substrate-binding pocket include Val80, Leu83, Ile106, Gly107, and Phe171 (Figs. 1A, 2A), with Val80 and Leu83 being well positioned to interact with the propanoic acid methyl group. The terminal carbon atom (CZ) of the Phe171 side chain is 4.1 Å from the phenoxy group of (*R*)-mecoprop; since LigPlot has a 4.0 Å threshold for hydrophobic interactions, this interaction is missed in Figure 2A.

To directly test the importance of potential substrate-binding residues of RdpA identified by the homology modeling and substrate docking procedures, variant forms of the enzymes were created by site-directed mutagenesis. To eliminate the bulky and polar Tyr221 and Arg285 residues, Y221A and R285A mutants were generated. In the presumed "hydrophobic pocket," Val80, Leu83, Ile106, and Phe171 each were changed to alanine to reduce hydrophobic interactions and thereby decrease the binding

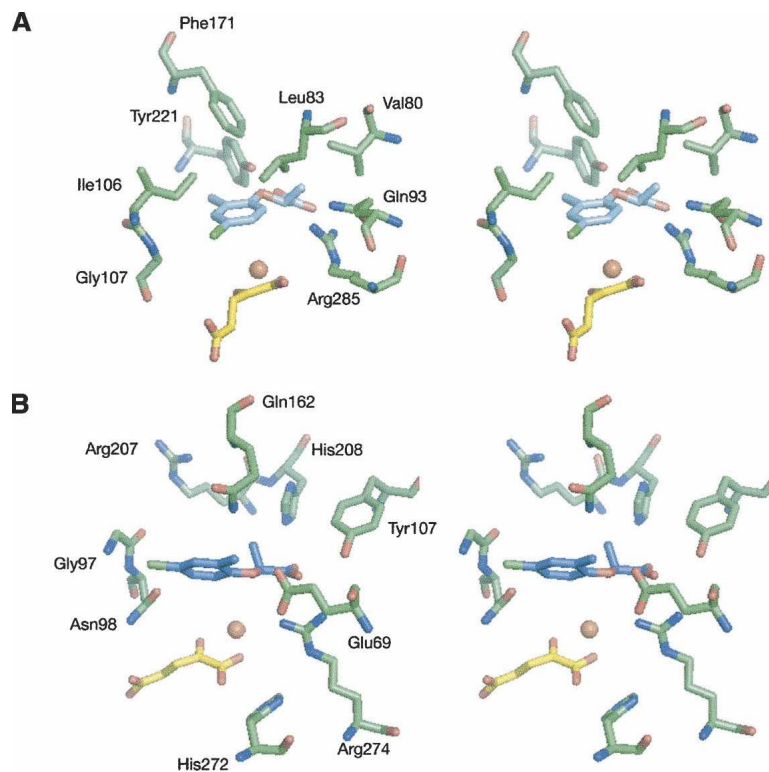


**Figure 1.** Stereo views of the most favorable models of the active sites of RdpA (A) and SdpA (B) with bound substrates. Shown are selected protein residues that are predicted to interact with the substrate. For clarity reasons, the Fe<sup>II</sup> ligands are not depicted. (*R*)- and (*S*)-mecoprop are indicated in light blue and in turquoise, respectively, and  $\alpha$ KG in yellow.

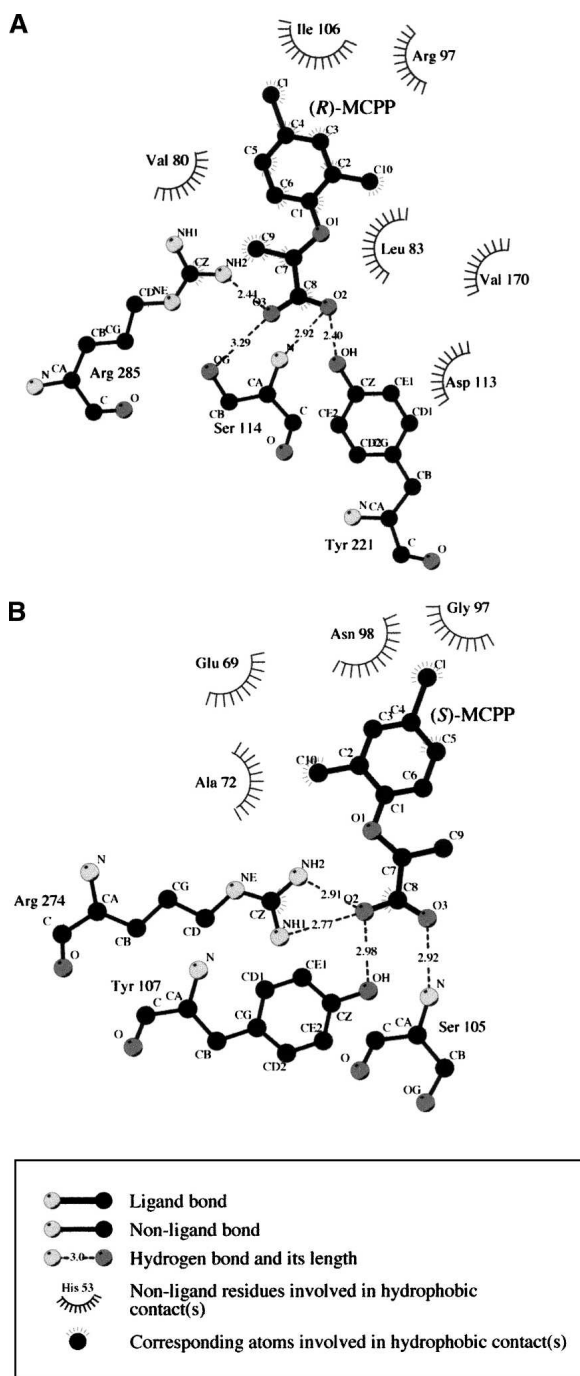


**Figure 2.** LIGPLOT diagrams of the active site models of RdpA (A) and SdpA (B). Shown are the most important interactions between the substrate and the active site according to the model.

affinity of (*R*)-mecoprop to the active site. Replacing Gly107—positioned near and coplanar with the phenoxy ring—with a bulkier hydrophobic residue is expected to hinder substrate binding, so this residue was mutated to Ile and Asn in the double mutants I106G/G107I and I106G/G107N, respectively.

The specific activities of the RdpA variants were tested using (*R*)-mecoprop and the racemic mixture (Table 1). The (*S*) enantiomer is not sold commercially and was available in very limited supply, so the RdpA variants were not tested with this compound. When the RdpA variants were examined using 4 mM (*R*)-mecoprop, the V80A and F171A variants exhibited ~60% of wild-type enzyme activity; I106A had ~30% of that activity and L83A, Y221A, and R285A were ~10% active. The activities of the double mutants I106G/G107I and I106G/G107N were further reduced compared with that of I106A, consistent with a bulkier side chain at position 107 presenting steric hindrance to substrate binding in a reactive conformation.

The RdpA variants retaining at least 10% of wild-type enzyme activity were subjected to more detailed kinetic characterization (Table 2). The maximal concentration of substrates that could be tested was 4 mM due to solubility limitations; therefore,  $K_m$  values higher than 800  $\mu\text{M}$  are only approximations and possess large errors. The  $K_m$  values of V80A and R285A RdpA variants were at least fivefold increased over that of the wild-type enzyme, whereas that of the I106A RdpA variant was more than 20-fold greater, supporting the described docking orientation of the model. The effect on the R285A variant can be understood in terms of decreased interaction with the substrate carboxylate, while the changes observed for the V80A and I106A variants are likely to arise from loss of hydrophobic interactions. The F171A protein had a threefold lower  $K_m$ , indicating either that this residue does not interact specifically with the phenoxy ring of (*R*)-mecoprop or that F171 is actually slightly hindering (*R*)-mecoprop binding. The calculated  $k_{\text{cat}}$  of all mutant proteins was similar to the wild-type value with the exception of the R285A mutant enzyme. Arg285 is postulated to interact with both the mecoprop carboxylate and the C-1 carboxylate of  $\alpha\text{KG}$ , so it could directly influence catalysis.

#### Binding of (*S*)-mecoprop to SdpA

The most favorable orientation of (*S*)-mecoprop was obtained with  $\alpha\text{KG}$  in the twist conformation in SdpA and (*S*)-mecoprop bound as illustrated in Figure 1B (with the corresponding ligand interactions shown in Fig. 2B). In this model, the substrate carboxylate interacts with the amide nitrogen of Ser105, the hydroxyl group of Tyr107, and the guanidino nitrogens of Arg274. Additional active site residues near the polar carboxylate include His272 and His208. Also of interest, the substrate ether oxygen atom is predicted to lie within 3.4 Å of the two carboxyl oxygens of Glu69. If protonated or bridged by the proton of a bound water molecule, the Glu69 carboxyl group could confer specificity to the (*S*) enantiomer by making a hydrogen bond with the ether oxygen (a prediction not borne out by experimental results, *vide infra*). Residues predicted to be

# Explore Litigation Insights

Docket Alarm provides insights to develop a more informed litigation strategy and the peace of mind of knowing you're on top of things.

## Real-Time Litigation Alerts



Keep your litigation team up-to-date with **real-time alerts** and advanced team management tools built for the enterprise, all while greatly reducing PACER spend.

Our comprehensive service means we can handle Federal, State, and Administrative courts across the country.

## Advanced Docket Research



With over 230 million records, Docket Alarm's cloud-native docket research platform finds what other services can't. Coverage includes Federal, State, plus PTAB, TTAB, ITC and NLRB decisions, all in one place.

Identify arguments that have been successful in the past with full text, pinpoint searching. Link to case law cited within any court document via Fastcase.

## Analytics At Your Fingertips



Learn what happened the last time a particular judge, opposing counsel or company faced cases similar to yours.

Advanced out-of-the-box PTAB and TTAB analytics are always at your fingertips.

## API

Docket Alarm offers a powerful API (application programming interface) to developers that want to integrate case filings into their apps.

## LAW FIRMS

Build custom dashboards for your attorneys and clients with live data direct from the court.

Automate many repetitive legal tasks like conflict checks, document management, and marketing.

## FINANCIAL INSTITUTIONS

Litigation and bankruptcy checks for companies and debtors.

## E-DISCOVERY AND LEGAL VENDORS

Sync your system to PACER to automate legal marketing.